

# Lightweight Borohydrides Electro-Activity in Lithium Cells

## Authors:

Daniele Meggiolaro, Luca Farina, Laura Silvestri, Stefania Panero, Sergio Brutti, Priscilla Reale

Date Submitted: 2018-11-27

Keywords: conversion reactions, negative electrodes, borohydrides, lithium-ion batteries

## Abstract:

As a substitute for graphite, the negative electrode material commonly used in Li-ion batteries, hydrides have the theoretical potential to overcome performance limits of the current state-of-the-art Li-ion cells. Hydrides can operate through a conversion process proved for some interstitial hydrides like  $MxHy + n Li = x M + y Li_mA$ , where  $m = n/y$ . Even if far from optimization, outstanding performances were observed, drawing the attention to the whole hydride family. Looking for high capacity systems, lightweight complex metal hydrides, such as borohydrides, deserve consideration. Capacities in the order of 2000-4000 mAh/g can be theoretically expected thanks to the very low formula unit weight. Although the potential technological impact of these materials can lead to major breakthroughs in Li-ion batteries, this new research field requires the tackling of fundamental issues that are completely unexplored. Here, our recent findings on the incorporation of borohydrides are presented and discussed.

Record Type: Published Article

Submitted To: LAPSE (Living Archive for Process Systems Engineering)

Citation (overall record, always the latest version):

LAPSE:2018.0972

Citation (this specific file, latest version):

LAPSE:2018.0972-1

Citation (this specific file, this version):

LAPSE:2018.0972-1v1

DOI of Published Version: <https://doi.org/10.3390/en9040238>

License: Creative Commons Attribution 4.0 International (CC BY 4.0)

Article

# Lightweight Borohydrides Electro-Activity in Lithium Cells

Daniele Meggiolaro <sup>1,2</sup>, Luca Farina <sup>1</sup>, Laura Silvestri <sup>1</sup>, Stefania Panero <sup>1</sup>, Sergio Brutti <sup>2,3,\*</sup> and Priscilla Reale <sup>4,\*</sup>

<sup>1</sup> Chemistry Department, Sapienza University, Piazzale Aldo Moro 5, Rome 00185, Italy; daniele.meggiolaro@uniroma1.it (D.M.); luca.farina@uniroma1.it (L.F.); laura.silvestri@uniroma1.it (L.S.); stefania.panero@uniroma1.it (S.P.)

<sup>2</sup> Istituto dei Sistemi Complessi, Consiglio Nazionale delle Ricerche (ISC-CNR), via dei Taurini, Rome 00185, Italy

<sup>3</sup> Dipartimento di Scienze, Università della Basilicata, v.le Ateneo Lucano 10, Potenza 85100, Italy

<sup>4</sup> Agenzia nazionale per le nuove tecnologie, l'energia e lo sviluppo economico sostenibile, ENEA, Centro Ricerche Casaccia, via Anguillarese 301, Rome 00123, Italy

\* Correspondence: sergio.brutti@unibas.it (S.B.); priscilla.reale@enea.it (P.R.); Tel.: +39-0971-205455 (S.B.); +39-06-30483248 (P.R.)

Academic Editor: Izumi Taniguchi

Received: 13 January 2016; Accepted: 15 March 2016; Published: 25 March 2016

**Abstract:** As a substitute for graphite, the negative electrode material commonly used in Li-ion batteries, hydrides have the theoretical potential to overcome performance limits of the current state-of-the-art Li-ion cells. Hydrides can operate through a conversion process proved for some interstitial hydrides like  $MgH_2$ :  $M_xA_y + n Li = x M + y Li_mA$ , where  $m = n/y$ . Even if far from optimization, outstanding performances were observed, drawing the attention to the whole hydride family. Looking for high capacity systems, lightweight complex metal hydrides, such as borohydrides, deserve consideration. Capacities in the order of 2000–4000 mAh/g can be theoretically expected thanks to the very low formula unit weight. Although the potential technological impact of these materials can lead to major breakthroughs in Li-ion batteries, this new research field requires the tackling of fundamental issues that are completely unexplored. Here, our recent findings on the incorporation of borohydrides are presented and discussed.

**Keywords:** lithium-ion batteries; negative electrodes; borohydrides; conversion reactions

## 1. Introduction

Lithium-ion batteries are the energy storage devices of choice for electric vehicles and smart grids based on renewable power sources; nevertheless, important efforts are still underway in the direction of new electrode materials capable to improve energy density, cycle life, cost effectiveness, and safety [1].

As substitutes for graphite, the negative electrode material commonly used in lithium-ion batteries, hydrides have the theoretical potential to overcome performance limits of the current state-of-the-art Li-ion cells [2]. Graphite has a maximum specific capacity of 372 mAh/g and operates in Li-ion batteries according to a multistep intercalation process, largely evolving at potential very close to 0 Volts *vs.*  $Li^+/Li^0$ ; thus, lithium metal deposition is a serious hazard that can occur when the battery is charged at high rate.

Hydrides can theoretically ensure much higher capacity values, operating through a conversion process (Hydride Conversion Reaction, HCR) according to the scheme:  $M_xA_y + n e^- + n Li^+ = x M^0 + y Li_mA$ , where  $e^-$  and  $Li^+$  are the electron and the lithium-ion, respectively, and  $m = n/y$  [2]. The improvement of the theoretical capacity is due to the multielectron redox process typical of conversions [2]. Hydride conversion reactions have been proved to occur in a safe potential range (*i.e.*, above 0.1 V)

for several covalent or interstitial hydrides like  $\text{MgH}_2$ ,  $\text{TiH}_2$  and  $\text{Mg}_2\text{NiH}_4$ , [2,3] and even if the optimization has not yet been pursued, outstanding performances have been already observed, enough to draw attention to the whole hydride family. The case of  $\text{MgH}_2$  is particularly appealing, since it boasts a theoretical specific capacity of 2048 mAh/g, and in the first cycle up to 1064 mAh/g, have already been delivered in the voltage range 1.0–0.1 V vs.  $\text{Li}^+/\text{Li}^0$ .

Looking for high capacity systems, light-weight complex metal hydrides, *i.e.*, alanates and borohydrides, deserve particular consideration. Through a full reduction to metallic elements and LiH, specific capacity values on the order of 2000–4000 mAh/g can be theoretically obtained thanks to the very low formula unit weight. Table 1 reports the theoretical capacity values that can be expected from light-weight borohydrides conversion. Indeed, we recently published how alanates in a lithium cell can sustain a full conversion reaction, and reversibility is mainly compromised by volume variation occurring upon reduction and the huge overpotential [4]. Although the potential technological impact of these materials can lead to major breakthroughs in Li-ion batteries, this new research field requires tackling fundamental issues that are completely unexplored.

**Table 1.** Borohydrides under investigation: structure and theoretical capacities.

Hydride	Symmetry	Theoretical Capacity/mAhg <sup>-1</sup>
$\text{LiBH}_4$	Pnma	4992
$\text{NaBH}_4$	Fm $\bar{3}$ m	2834
$\text{KBH}_4$	Fm $\bar{3}$ m	1987
$\text{Mg}(\text{BH}_4)_2$	P6 <sub>1</sub> 22	3971
$\text{Ca}(\text{BH}_4)_2$	$\alpha$ Fddd	3074

Borohydrides are polyanionic materials in which hydrogen is covalently bonded to central atoms in “complex” anions. Thanks to their high hydrogen gravimetric densities, they are considered valuable candidates as hydrogen storage materials. Nevertheless, hitherto, they have mainly been used as “one pass” storage systems, in which hydrogen is evolved upon the highly irreversible water hydrolysis [5,6]. In fact, high kinetic barriers preclude their dehydrogenation and/or rehydrogenation in the solid state. Recently, great research efforts have been made in the attempt to overcome them through catalytic doping, nano-engineering, additive destabilization and chemical modification [7–9].

On the other hand, if the kinetic stability of borohydrides to hydrogen desorption is a problematic issue in the hydrogen storage field, it could be an advantage in view of the possible application as electrodes in lithium-ion batteries, where the gas evolution would be a serious hazard. Conceivable conversion reactions of borohydrides somehow remind the thermal hydrogen desorption/adsorption processes, but differ in the final destination of hydrogen, that is not oxidized but forms lithium hydride. In this perspective, neither the thermodynamic nor the kinetic feasibility of these reactions can be easily predicted. A preliminary evaluation of their theoretical capacities supplied in full lithium conversion reactions are summarized in the Table 1, thus suggesting the remarkable potential of these materials as high capacity anodes in Li cells.

Here, we report our recent findings about the incorporation of light-weight borohydrides in a lithium cell. This is the first ever reported investigation about the incorporation of these materials as candidate negative electrodes in secondary lithium cells. This study has been carried out by a combined computational and experimental approach. Density Functional Theory (DFT) calculations have been performed in order to preliminarily verify the thermodynamics of the hydride conversion reactions. The subsequent experimental work focuses on the characterization of the basic chemical-physical features and testing the real behavior in electrochemical lithium cells. In the last section, some general conclusions are drawn.

## 2. Computational and Experimental Details

DFT calculations in generalized-gradient-approximation (GGA-PBE) [10] with projector augmented wave (PAW) potentials [11] and planewaves were performed to predict the expected

potential *vs.* Li of the possible conversion reactions involving  $M(\text{BH}_4)_x$  and  $\text{MH}_x$  phases, where  $x$  is equal to 1 for Li, Na and K and 2 for Mg and Ca. Structural parameters of all the borohydrides, metal hydrides and metallic elements involved in the possible envisaged reactions were computed. The kinetic energy cutoff was fixed at 500 eV and Monkhorst-Pack uniform  $k$ -points meshes in the Brillouin Zone (BZ) have been adopted for all the computed lattices, in order to achieve a final computational accuracy of 2 meV  $\text{at}^{-1}$  on the total energy. The equilibrium structures of the lattices have been found relaxing both cells and ion positions until forces acting on atoms were less than  $10^{-3}$  eV/Å. All calculations were carried out by using the VASP 5.2 code [12]. The energetics at 0 K were evaluated for each reaction and the associated cell voltage  $\Delta V$  was calculated according to the general relation  $\Delta V = -\Delta_r E/nF$ , where  $\Delta_r E$  is the total energy of reaction as obtained by the DFT calculations,  $n$  the number of exchanged electrons in the reaction and  $F$  the Faraday constant.

Borohydrides used in this studied were purchased from Aldrich (St. Louis, MO, USA) ( $\text{LiBH}_4 \geq 90\%$ ,  $\text{NaBH}_4$  99%,  $\text{KBH}_4$  99.9%,  $\text{Mg}(\text{BH}_4)_2$  95%,  $\text{Ca}(\text{BH}_4)_2$  purity not defined) and were not subjected to any purification. All manipulations were performed in an Argon filled glove box, with controlled humidity and oxygen content.

Mechanochemical activation treatments were performed on all borohydrides by means of a M400 Spex Shaker (SPEX SamplePrep, Metuchen, NJ, USA), in stainless steel jars, with 10 mm diameter stainless steel balls and a powder to balls weight ratio 1:20. All treatments consisted of 1 or 15 h of grinding of pure borohydrides. In the case of the materials used in the electrochemical tests, a further mechanochemical treatment was performed for 0.5 or 5 h of milling, and for the 1 or 15 h pre-milled samples, respectively, with the conductive carbon Super P in a 5:3 weight ratio, in order to achieve an intimate mixing.

The effect of milling on structure and particles morphology was evaluated by X-ray powder diffraction (XRD) and tunneling electron microscopy. XRD patterns were collected in borosilicate capillary sample holder in a Rigaku Ultima+ Diffractometer (Rigaku Corporation, Tokyo, Japan), equipped with Cu  $K\alpha$  source in a theta-theta Bragg–Brentano geometry. Reference structures from Inorganic Crystal Structure Database (ICSD) were used for phase identification. Transmission electron microscopy (TEM) images were acquired by using an FEI Tecnai cryo-TEM instrument (FEI Company Hillsboro, Oregon, OR, USA) with an e-beam acceleration of 80 eV. Samples have been suspended by sonication in dried hexane and then spread on carbon filmed copper grids for microscopy.

For electrochemical tests, electrodes were prepared by adding PVdF Kynar 2801 (Arkema, Colombes, France) to the ball milled mixture of borohydrides and Super P (Imerys Graphite & Carbon, Bodio, Switzerland), in order to get an active material/SuperP/polymer weight ratio of 5/3/2. The final mixture was pressed on 10 mm diameter Cu disks with a mild pressure, in order to obtain electrodes with around 1–2  $\text{mg}/\text{cm}^2$  active material.

Assembled electrochemical cells were 12 mm coin cells, where the electrode was faced to a lithium metal foil through a Whatmann borosilicate fiber separator (Whatmann, Maidstone, UK) swollen with a 1 M electrolyte solution of  $\text{LiPF}_6$  in ethylene carbonate—dimethyl carbonate (EC:DMC) 1:1 mixture (LP30, Merk Selectipur).

Galvanostatic cycling tests were performed by means of a Maccor battery tester (Maccor, Tulsa, OK, USA), in the potential range of 2.5–0.01 V or 2.0–0.01 V at a rate equal to  $C/20$ , calculated as the current to deliver in 20 h the full theoretical conversion capacity.

### 3. Results and Discussion

#### 3.1. Density Functional Theory (DFT) Calculation Results

The equilibrium structures of the borohydrides phases are reported in the Figure 1. Details about the structural parameters obtained by the DFT optimization procedure have been reported in Table 2. In all the borohydrides phases, the alkali metal ions are coordinated by  $\text{BH}_4^-$  units where the B atoms are tetrahedrally coordinated by 4 H atoms at distances of 1.20–1.23 Å.

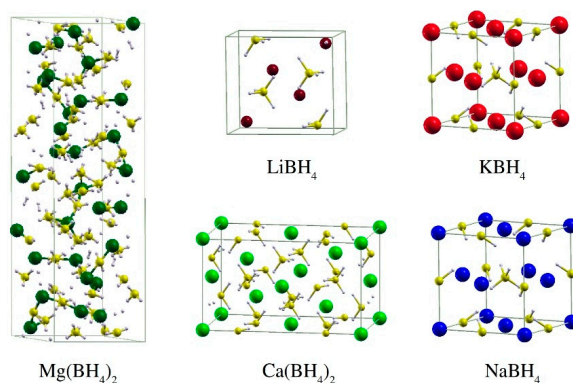


**Figure 1.** Crystal structures of the borohydrides phases.

**Table 2.** Borohydrides under investigations: structure and theoretical capacity.

Hydride	Crystal Structure	Wickoff Positions
LiBH <sub>4</sub>	Space group (SG): Pnma a = 7.179 Å, b = 4.425 Å c = 6.784 Å α = β = γ = 90°	Li 4c 0.3432 0.2500 0.3922 B 4c 0.1913 0.2500 0.0750 H 4c 0.5890 0.2500 0.5700 H 4c 0.0990 0.2500 0.2278 H 8d 0.7076 0.5277 -0.0740
α-NaBH <sub>4</sub>	SG: Fm3m a = b = c = 6.061 Å α = β = γ = 90°	Na 4a 0.0000 0.0000 0.0000 B 4b 0.5000 0.5000 0.5000 H 32f 0.3779 0.3779 0.3779 (SOF = 0.5)
α-KBH <sub>4</sub>	SG: Fm3m a = b = c = 6.720 Å α = β = γ = 90°	K 4a 0.0000 0.0000 0.0000 B 4b 0.5000 0.5000 0.5000 H 32f 0.6116 0.6116 0.6116 (SOF = 0.5)
Mg(BH <sub>4</sub> ) <sub>2</sub>	SG: P6 <sub>1</sub> 22 a = b = 10.853 Å, c = 38,007 Å α = β = 90°, γ = 120°	Mg 12c 0.05054 0.38682 0.63466 Mg 12c 0.52433 0.49036 0.58645 Mg 6a 0.11473 0.00000 0.00000 B 12c 0.30046 0.44814 0.61632 B 12c 0.54901 0.72715 0.70086 B 12c -0.05929 0.12179 0.64803 B 12c -0.01609 0.46331 0.68983 B 6b 0.70779 0.41558 0.25000 B 6b 0.49167 -0.01666 0.25000 H 12c 0.50844 0.30049 0.60816 H 12c 0.66786 0.41723 0.56978 H 12c 0.09056 0.58004 0.60953 H 12c -0.07431 0.37521 0.59175 H 12c 0.26859 0.49322 0.64430 H 12c 0.18881 0.36797 0.59804 H 12c 0.36242 0.37676 0.62526 H 12c 0.38660 0.56156 0.59823 H 12c 0.66970 -0.05463 0.62669 H 12c 0.82885 0.73122 0.62880 H 12c 0.63200 0.58491 0.63222 H 12c 0.71208 0.70335 0.59113 H 12c 0.84007 0.04825 0.67057 H 12c -0.02929 0.03889 0.62994 H 12c 0.05388 0.21536 0.66407 H 12c 0.89141 0.18147 0.62707 H 12c 0.09752 0.53656 0.67085 H 12c 0.87539 0.37479 0.67144 H 12c -0.04600 0.55408 0.70426 H 12c 0.01070 0.39214 0.71266
Ca(BH <sub>4</sub> ) <sub>2</sub>	SG: Fddd a = 8.737 Å, b = 13.062 Å, c = 7.477 Å α = β = γ = 90°	Ca 8a 0.0000 0.0000 0.0000 B 16f 0.0000 0.2227 0.0000 H 32h 0.8869 0.2773 0.0112 H 32h 0.0001 0.1693 0.1357

The standard pressure/room temperature polymorph of the  $\text{LiBH}_4$  phase has an orthorhombic cell (s.g. Pnma) [13] with lattice parameters  $a = 7.179 \text{ \AA}$ ,  $b = 4.425 \text{ \AA}$  and  $c = 6.784 \text{ \AA}$ . In the cell, four unit formulas of  $\text{LiBH}_4$  are present where the  $\text{Li}^+$  cations are coordinated by four  $\text{BH}_4^-$  units at a mean distance of  $2.53 \text{ \AA}$ . The tetrahedral  $\text{BH}_4^-$  anions are strongly distorted with respect to both bond distances and angles.

The  $\alpha\text{-NaBH}_4$  lattice is the standard pressure polymorph stable at room temperature of the sodium borohydride [14]. It crystallizes in a cubic NaCl-type cell (s.g. Fm3m) with  $a = b = c = 6.061 \text{ \AA}$ . In the cell, four formula units of the phase are present, with Na and B atoms in the 4a and 4b Wickoff positions respectively, while the H atoms occupy the 32f positions with occupancy factor of 0.5.  $\text{Na}^+$  cations are octahedrally coordinated by  $\text{BH}_4^-$  units at distances of  $3.03 \text{ \AA}$ .

The  $\alpha\text{-KBH}_4$  is isostructural with the  $\alpha\text{-NaBH}_4$  cubic phase and has lattice constants of  $a = b = c = 6.720 \text{ \AA}$  with four formula units per cell.  $\text{K}^+$  cations in the cell are octahedrally coordinated by  $\text{BH}_4^-$  units at a distance of  $3.36 \text{ \AA}$  [15].

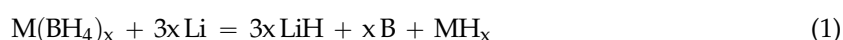
$\text{Mg}(\text{BH}_4)_2$  has a large hexagonal cell with  $a = b = 10.853 \text{ \AA}$  and  $c = 38.007 \text{ \AA}$  and 30 formula units, where the Mg cations are at distances of about  $2.40 \text{ \AA}$  from the  $\text{BH}_4^-$  tetrahedral [16,17].

$\text{Ca}(\text{BH}_4)_2$  crystallizes in an orthorhombic cell (s.g. Fddd) with  $a = 8.737 \text{ \AA}$ ,  $b = 13.062 \text{ \AA}$  and  $c = 7.477 \text{ \AA}$  and eight unit formulas. The metal cation Ca in the cell is coordinated by six  $\text{BH}_4^-$  units in distorted octahedra at distances of about  $2.90 \text{ \AA}$  [18].

Starting from the total energies of the equilibrium lattices of the borohydrides, metal hydrides and simple metals, the energetics and the associated potentials *vs.* Li of the conversion reactions of borohydrides in Li-cell have been calculated following the simple approach already used by us for  $\text{MgH}_2$  and alanates [4,19–21]. These predictions allow for evaluating the thermodynamic feasibility of borohydrides conversion upon reaction with lithium. It is worth noting that reaction schemes different from conversion are highly improbable. The atomic species constituting the hydrides under consideration are not transition metals, and, therefore, lithium insertion mechanisms are not possible. Borohydrides are not metallic materials, and as soon as reduction occurs, the covalent B-H bonds are compromised, the structure is destroyed and no substitution mechanism can be conceived.

Conversion reactions were hypothesized either as direct or as multistep processes.

A two-step mechanism can be envisaged, according to the following scheme:



On the contrary, in the direct process, the borohydride is in one pot reduced to LiH and metallic elements:



The predicted reaction energies and the associated potentials (*vs.* Li) of reactions (1)–(3) for all the studied borohydrides are reported in Table 3.

Calculations demonstrate the general thermodynamic feasibility of borohydrides conversion and that, apart for the cases of lithium calcium borohydride, both the direct and the two-step reactions paths are possible.

Lithium borohydride can react accordingly only to R1, and calculations demonstrate that it has the highest conversion electromotive force among the alkaline borohydrides, *i.e.*,  $0.42 \text{ V}$ .

**Table 3.** Predicted thermodynamics of the borohydrides hypothetical conversion reactions in lithium cells.

	Reaction	$\Delta E$ kJ/mol	Emf V vs. Li
R1	$\text{LiBH}_4 + 3 \text{Li} = \text{B} + 4 \text{LiH}$	−123.3	0.42
R2.1	$\text{NaBH}_4 + 3 \text{Li} = \text{NaH} + \text{B} + 3 \text{LiH}$	−91.7	0.32
R2.2	$\text{NaH} + \text{Li} = \text{Na} + \text{LiH}$	−41.6	0.43
R2.3	$\text{NaBH}_4 + 4 \text{Li} = \text{Na} + \text{B} + 4 \text{LiH}$	−133.4	0.34
R3.1	$\text{KBH}_4 + 3 \text{Li} = \text{KH} + \text{B} + 3 \text{LiH}$	−46.5	0.16
R3.2	$\text{KH} + \text{Li} = \text{K} + \text{LiH}$	−40.9	0.42
R3.3	$\text{KBH}_4 + 4 \text{Li} = \text{K} + \text{B} + 4 \text{LiH}$	−87.4	0.23
R4.1	$\text{Ca}(\text{BH}_4)_2 + 6 \text{Li} = 6 \text{LiH} + 2 \text{B} + \text{CaH}_2$	−262.4	0.45
R4.2	$\text{CaH}_2 + 2 \text{Li} = \text{Ca} + 2 \text{LiH}$	+3.2	−0.02
R4.3	$\text{Ca}(\text{BH}_4)_2 + 8 \text{Li} = 8 \text{LiH} + 2 \text{B} + \text{Ca}$	−259.2	0.33
R5.1	$\text{Mg}(\text{BH}_4)_2 + 6 \text{Li} = 6 \text{LiH} + 2 \text{B} + \text{MgH}_2$	−289.3	0.50
R5.2	$\text{MgH}_2 + 2 \text{Li} = \text{Mg} + 2 \text{LiH}$	−106.3	0.55
R5.3	$\text{Mg}(\text{BH}_4)_2 + 8 \text{Li} = 8 \text{LiH} + 2 \text{B} + \text{Mg}$	−395.6	0.51

For sodium, potassium and magnesium borohydrides, the full reductions to metallic elements and LiH, namely R2.3, R3.3, R5.3, respectively, appear to be slightly favored compared to the partial reductions in which the intermediate metal hydrides  $\text{MH}_x$  are formed, namely R2.2, R3.2, R5.2, respectively. However, it is to be noted that the differences between the two competitive mechanisms are in all cases smaller than 80 mV. Thus, the possible occurrence of thermodynamic overpotential as large as in the  $\text{MgH}_2$  conversion reaction (*i.e.*, 71 mV), may imply the possible occurrence of the two-step mechanism 1–2 instead of the thermodynamically favored single step one, *i.e.*, mechanism 3. On passing, it may be of interest to mention that magnesium borohydride conversion reaction may also involve the formation of metallic borides like  $\text{MgB}_2$  or other intermetallic phases [22,23] analogous to the hydrogen desorption reaction [24]. However, the borides' formation occurs at high temperature after the complete conversion from  $\text{Mg}(\text{BH}_4)_2$  to  $\text{MgH}_2$  as a second desorption step. In this view, and also considering the well-known mechanism of the conversion of  $\text{MgH}_2$  [2,25] to give  $\text{Mg} + \text{LiH}$ , we omitted investigating this point that, in our opinion, would be too speculative.

Turning to  $\text{Ca}(\text{BH}_4)_2$ , the slightly positive reaction energy, +3.2 kJ/mol, predicted for  $\text{CaH}_2$  conversion suggests that reaction R4.2 is thermodynamically unfavored in comparison to the lithium plating reaction, and calcium borohydride should convert only to CaH, B and LiH. The disadvantageous prediction on the conversion reaction of  $\text{CaH}_2$  in lithium cells is actually in agreement with unpublished experimental findings that we obtained in our laboratory.

It is worth noting that all the estimated electromotive forces, ranging between 200 and 500 mV, are values of great practical interest for Li-ion application. In fact, they are small enough to be suitable for negative electrodes in lithium-ion cells but at least 200 mV far from the thermodynamic potential of lithium plating, thus improving the intrinsic safety of the device.

### 3.2. Sample Preparation and Preliminary Characterization

Mechanochemical treatments are complex processes that generally result in a number of different positive effects [26]: (1) the particle size reduction; (2) the breaking of the oxide layers; (3) the induction of a high level of elastic shears and other stresses; and eventually (4) the formation of a stacking fault disorder and (5) the increase of the atomic disorder. For these reasons, as it is generally applied to activate hydrogen desorption, high energy ball milling was used to pretreat commercial borohydrides.

X-ray powder diffraction has been carried out on all the hydrides as purchased, and after 15 h mechanochemical activation treatments. Patterns are reported in Figure 2, where the background halo observed is due to the glass capillary used as holder in the experiments.

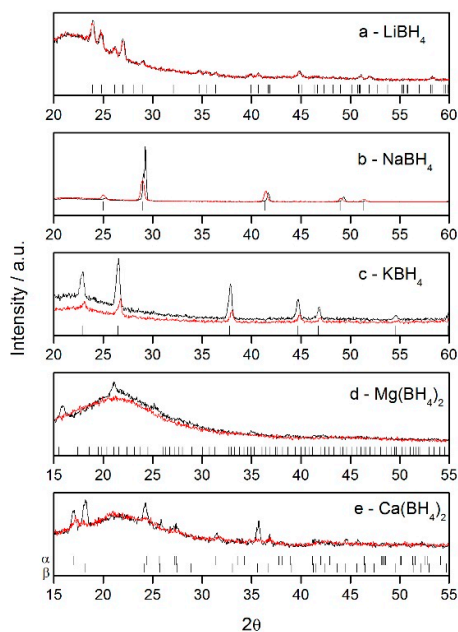


**Figure 2.** XRD analysis of  $\text{LiBH}_4$  (a);  $\text{NaBH}_4$  (b);  $\text{KBH}_4$  (c);  $\text{Mg}(\text{BH}_4)_2$  (d); and  $\text{Ca}(\text{BH}_4)_2$  (e) before (black line) and after 15 h mechanochemical treatment (red line).

Lithium borohydride perfectly matched the tetragonal  $\text{Pnma}$  structure described in the ICSD 245567 card, and it is hardly affected by the performed high energy ball milling. Sodium and potassium borohydrides both have a cubic symmetry, as reported in the 27861 and 27862 ICSD references respectively; upon milling, the reduction of peaks intensity can be observed, suggesting a certain nanometrization degree.

This effect is more marked for magnesium and calcium borohydrides. Pristine calcium borohydride demonstrates being a mix of its two  $\alpha$  orthorhombic (ICSD 166669) and  $\beta$  tetragonal (ICSD 166671) allotropes, whereas the as-purchased magnesium borohydride is poorly crystalline and even the unmilled pristine material shows only a few broad diffraction lines. Once milled,  $\text{Mg}(\text{BH}_4)_2$  and  $\text{Ca}(\text{BH}_4)_2$  become fully amorphous and XRD analysis show featureless patterns after the mechanochemical activation.

Figure 3a–e shows some TEM images collected for the pristine as purchased samples under investigation.

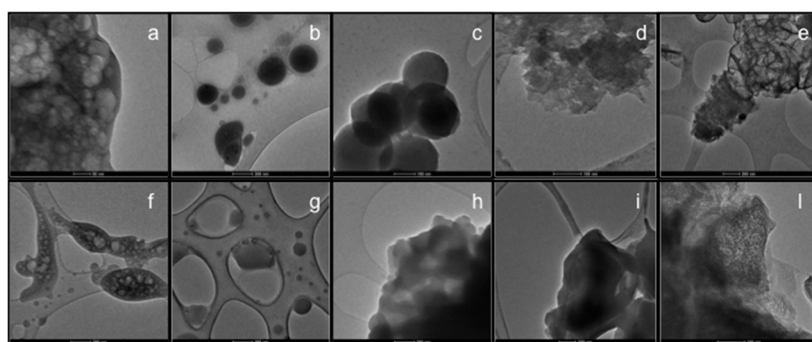


**Figure 3.** TEM images of pristine  $\text{LiBH}_4$  (a);  $\text{NaBH}_4$  (b);  $\text{KBH}_4$  (c);  $\text{Mg}(\text{BH}_4)_2$  (d);  $\text{Ca}(\text{BH}_4)_2$  (e); and 15 h mechanochemical treated  $\text{LiBH}_4$  (f);  $\text{NaBH}_4$  (g);  $\text{KBH}_4$  (h);  $\text{Mg}(\text{BH}_4)_2$  (i); and  $\text{Ca}(\text{BH}_4)_2$  (l).

Generally speaking, all these samples were extremely challenging in the electron microscope, with electron energies above 80 eV all hydrides largely interacting with the beam by melting and releasing hydrogen. Large voids were formed quickly wherever acceleration voltages as high as 200 kV were



used, as well as at large magnifications at 80 eV. In the last case, electrons were in fact concentrated in a very limited area of the samples thus leading to massive damages of the morphology. Such behavior limited the use of the TEM technique to the low-to-mid magnification range.

All alkaline borohydrides were characterized by a similar morphology of pseudo-spherical particles with diameters in the range 100–200 nm.  $\text{LiBH}_4$  particles were very reactive under the electron beam event at 80 eV of acceleration voltage. In fact, the spherical particles easily and quickly melted/reacted by releasing gas, thus forming round voids throughout the entire illuminate area. On the contrary,  $\text{Mg}(\text{BH}_4)_2$  and  $\text{Ca}(\text{BH}_4)_2$  presented aggregates of very small nanometric particles with an inhomogeneous shape. In particular, in the  $\text{Ca}(\text{BH}_4)_2$  sample, two different morphologies were observed—small irregular nanoparticles with size in the 10–20 nm range and large almost transparent spherical particles with grain size ranging between 100 and 300 nm. These two morphologies are likely due to the two polymorphs observed in the XRD analysis.

The effect of the milling for 15 h on the borohydrides morphology is complex, see Figure 3f–l. The mechanochemical treatment in the case of Li and Na borohydrides led to the pulverization of the pristine particles that reduced in size. In the case of K, Mg and Ca borohydrides, it produced the formation of large homogeneous aggregates—the latter effect is particularly relevant in the case of  $\text{Mg}(\text{BH}_4)_2$ .

For this reason, the effect of a shorter mechanochemical activation treatment has been verified in the two very different cases of magnesium and sodium borohydride. Both pristine materials were mechanochemically pretreated only for 1 h: XRD were collected and morphology observed. Data are not shown, but it was found that 1 h of milling left the  $\text{NaBH}_4$  material unaltered, both structurally and morphologically compared to the pristine state. On the contrary, in the case of  $\text{Mg}(\text{BH}_4)_2$ , even this short treatment was sufficient to destroy any crystallinity and produce a wide particle coalescence, although to a lower extent in respect to the 15 h treatment.

### 3.3. Electrochemical Tests

Galvanostatic cycling tests were performed to finally verify the electrochemical activity of the borohydrides under investigation in lithium cells. Figure 4 reports the voltage profiles for two discharge-charge cycles of the borohydrides milled for 15 + 5 h with Super P carbon.

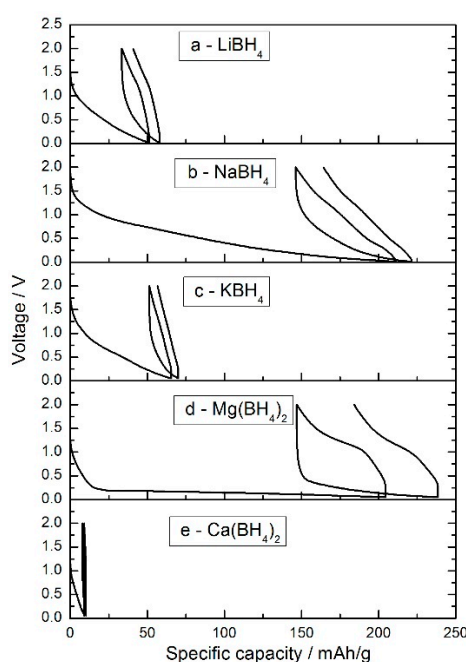


**Figure 4.** Galvanostatic discharge/charge voltage profiles of 15 + 5 h mechanochemical treated  $\text{LiBH}_4$  (a);  $\text{NaBH}_4$  (b);  $\text{KBH}_4$  (c);  $\text{Mg}(\text{BH}_4)_2$  (d); and  $\text{Ca}(\text{BH}_4)_2$  (e).

$\text{Ca}(\text{BH}_4)_2$  appears to be completely electrochemically inactive in addition to  $\text{LiBH}_4$  and  $\text{KBH}_4$ , which showed an almost negligible reactivity, the first discharge capacity being less than 5% of the theoretical one in all cases. This poor electrochemical activity could be possibly ascribed to limited electron/ionic conductivity or high activation energy of the conversion reaction, thus reflecting large kinetics overpotential. It is likely that some of these possible drawbacks may be mitigated by a careful tuning of the sample morphology, like in the case of nano- $\text{MgH}_2$  particles deposited onto carbonaceous matrix [27]. However, such a complex synthetic strategy is beyond the scope of this manuscript.

Slightly more encouraging are the performances of  $\text{NaBH}_4$  and  $\text{Mg}(\text{BH}_4)_2$ , which can exchange more than 200 mAh/g upon the first reduction. Looking more into the details of the shape of the voltage profiles, it must be noted that, among all the samples under investigation, only magnesium borohydride showed a rather defined process in a region compatible with the predicted conversion potentials, *i.e.*, below 0.5 V *vs.* Li. In fact, the reactivity of the sodium borohydride sample extends from 1 V to 0 V *vs.* lithium, thus making the interpretation of this featureless lithium loading slope very difficult.

However, for both of the active borohydrides, in order to verify the effect of the mechanochemical treatment on the delivered electrochemical performances, materials mechanochemically treated for 1 h and then milled with super P 30 min were also tested in lithium cells. Figures 5 and 6 show a comparison between the performances obtained with different mechanochemical treatments.

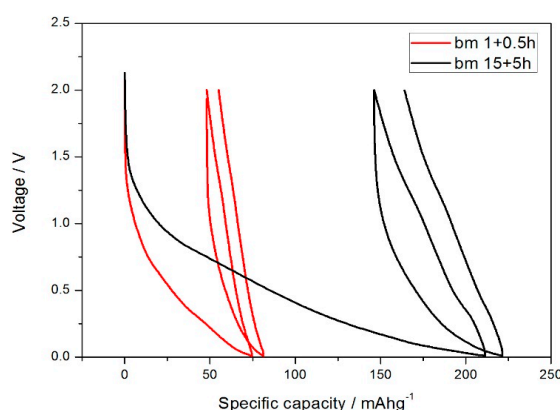


**Figure 5.** Comparison of galvanostatic discharge/charge voltage profiles  $\text{NaBH}_4$  after 1 + 0.5 h (red line) and after 15 + 5 h (black line) milling.

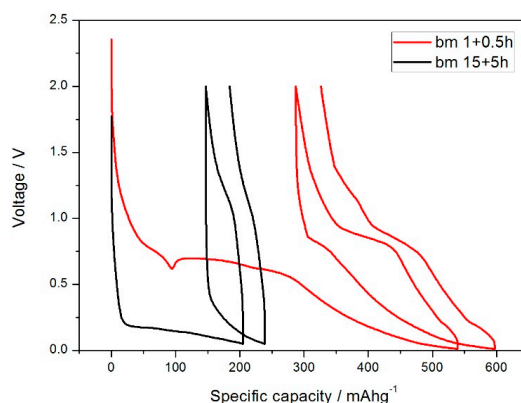


**Figure 6.** Comparison of galvanostatic discharge/charge voltage profiles  $\text{Mg}(\text{BH}_4)_2$  after 1 + 0.5 h (red line) and after 15 + 5 h (black line) milling.

As already noticed in the structural and morphological characterization of the samples, the effect of milling length on the performances in lithium cells is markedly different for the two borohydrides.

In the case of  $\text{NaBH}_4$ , where the crystallinity is kept upon milling, the longer the mechanochemical treatment, the more extended is the particle size reduction and the larger the capacity upon reduction.

On the contrary, the performances of  $\text{Mg}(\text{BH}_4)_2$  in lithium cells are improved by a shorter mechanochemical treatment. Beneath the crystallinity is very poor in the pristine state and totally lost even after a very short milling, the reduced particles' coalescence likely plays a significant role. In fact, the first discharge capacity is increased by the 270% reaching 540 mAh/g, and about 250 mAh/g are exchanged during the following re-charge process. In addition, the voltage profile is largely modified: the redox activity evolves at the least through two processes, at around 0.7 and 0.2 V.

The possibility of multiple overlapping reactions, discussed in the computational results section, is expected. Nevertheless, the first step voltage value, 0.7 V, does not match with the DFT calculation. Further investigations are needed to shed light on the reaction path interpretation. As a mere speculation, one may also consider the possible occurrence of mixed borohydride upon reduction, similarly to what was observed by us and by Latroche and co-workers for sodium alanate conversions [21,28].

#### 4. Conclusions

In summary, in this communication, we have reported for the first time in the literature a study about the electrochemical activity in Li-ion cells of borohydrides. Even if the experimental capacities obtained are far from the theoretical ones, the  $\text{NaBH}_4$  and  $\text{Mg}(\text{BH}_4)_2$  performances suggest that the electrochemical activity exists and can be tuned by altering the sample morphology, the optimal condition apparently consisting in small and poorly aggregate crystalline particles. In this view and considering what was already experienced in the case of many other electrode materials for Li-ion cells [29–31], possible large improvements in the performances can be achieved by the optimization of the sample morphology, especially by a fine tuning of nanostructure and phase mixing at the nanoscale. The synthesis of samples with controlled morphology at the nanoscale is under investigation at present.

**Acknowledgments:** This work is carried out under the framework of the Italian project (FIRB—Futuro in ricerca 2010) “Hydrides as high capacity anodes for lithium-ion batteries”.

**Author Contributions:** Laura Silvestri and Priscilla Reale synthesized and characterized the samples. Luca Farina and Stefania Panero carried out the electrochemical investigation, and Sergio Brutti and Daniele Meggiolaro completed the computational study. Priscilla Reale and Sergio Brutti wrote the manuscript.

**Conflicts of Interest:** The authors declare no conflict of interest.

#### References

1. Scrosati, B.; Garche, J. Lithium batteries: Status, prospects and future. *J. Power Sources* **2010**, *1995*, 2419–2430. [[CrossRef](#)]
2. Oumellal, Y.; Rougier, A.; Nazri, G.; Tarascon, J.; Aymard, L. Metal hydrides for lithium-ion batteries. *Nat. Mater.* **2008**, *7*, 916–921. [[CrossRef](#)] [[PubMed](#)]
3. Vitucci, F.M.; Paolone, A.; Brutti, S.; Munaò, D.; Silvestri, L.; Panero, S.; Reale, P.  $\text{H}_2$  thermal desorption and hydride conversion reactions in Li cells of  $\text{TiH}_2/\text{C}$  amorphous nanocomposites. *J. Alloys Compd.* **2015**, *645*, S46–S50. [[CrossRef](#)]
4. Silvestri, L.; Forgia, S.; Farina, L.; Meggiolaro, D.; Panero, S.; La Barbera, A.; Brutti, S.; Reale, P. Lithium alanates as negative electrode in lithium ion batteries. *ChemElectroChem* **2015**, *2*, 877–886. [[CrossRef](#)]
5. Orimo, S.-I.; Nakamori, Y.; Eliseo, J.R.; Züttel, A.; Jensen, C.M. Complex hydrides for hydrogen storage. *Chem. Rev.* **2007**, *107*, 4111–4132. [[CrossRef](#)] [[PubMed](#)]
6. Yadav, M.; Xu, Q. Liquid-phase chemical hydrogen storage materials. *Energy Environ. Sci.* **2012**, *5*, 9698–9725. [[CrossRef](#)]
7. Li, C.; Peng, P.; Zhou, D.W.; Wan, L. Research progress in  $\text{LiBH}_4$  for hydrogen storage: A review. *Int. J. Hydrogen Energy* **2011**, *36*, 14512–14526. [[CrossRef](#)]
8. Muir, S.S.; Yao, X. Progress in sodium borohydride as a hydrogen storage material: Development of hydrolysis catalysts and reaction systems. *Int. J. Hydrogen Energy* **2011**, *36*, 5983–5997. [[CrossRef](#)]

9. Newhouse, R.J.; Stavila, V.; Hwang, S.-J.; Klebanoff, L.E.; Zhang, J.Z. Reversibility and improved hydrogen release of magnesium borohydride. *J. Phys. Chem. C* **2010**, *114*, 5224–5232. [[CrossRef](#)]
10. Perdew, J.P.; Burke, K.; Ernzerhof, M. Generalized gradient approximation made simple. *Phys. Rev. Lett.* **1996**, *77*, 3865. [[CrossRef](#)] [[PubMed](#)]
11. Joubert, D.; Kresse, G. From ultrasoft pseudopotentials to the projector augmented-wave method. *Phys. Rev. B* **1999**, *59*, 1758.
12. Kresse, G.; Hafner, J. Ab initio molecular dynamics for liquid metals. *Phys. Rev. B* **1993**, *47*, 558. [[CrossRef](#)]
13. Soulié, J.-P.; Renaudin, G.; Cerny, R.; Yvon, K. Lithium boro-hydride LiBH<sub>4</sub>: I. Crystal structure. *J. Alloys Compd.* **2002**, *346*, 200–205. [[CrossRef](#)]
14. Damian, G.A.; Hudson, B.S. Inelastic neutron scattering spectra of NaBH<sub>4</sub> and KBH<sub>4</sub>: reproduction of anion mode shifts via periodic DFT. *Chem. Phys. Lett.* **2004**, *385*, 166–172.
15. Vajeeston, P.; Ravindran, P.; Kjekshus, A.; Fjellvag, H. Structural stability of alkali boron tetrahydrides ABH<sub>4</sub> (A = Li, Na, K, Rb, Cs) from first principle calculation. *J. Alloys Compd.* **2005**, *387*, 97–104. [[CrossRef](#)]
16. Cerny, R.; Filinchuk, Y.; Hagemann, H.; Yvon, K. Magnesium borohydride: Synthesis and crystal structure. *Angew. Chem.* **2007**, *119*, 5867–5869. [[CrossRef](#)]
17. Her, J.H.; Stephens, P.W.; Gao, Y.; Soloveichik, G.L.; Rijssenbeek, J.; Andrus, M.; Zhao, J.C. Structure of unsolvated magnesium borohydride Mg(BH<sub>4</sub>)<sub>2</sub>. *Acta Crystallogr. B* **2007**, *63*, 561–568. [[CrossRef](#)] [[PubMed](#)]
18. Miwa, K.; Aoki, M.; Noritake, T.; Ohba, N.; Nakamori, Y.; Towata, S.; Zuttel, A.; Orimo, S. Thermodynamical stability of calcium borohydride Ca(BH<sub>4</sub>)<sub>2</sub>. *Phys. Rev. B* **2006**, *74*, 155122–155126. [[CrossRef](#)]
19. Meggiolaro, D.; Gigli, G.; Paolone, A.; Vitucci, F.; Brutti, S. Incorporation of lithium by MgH<sub>2</sub>: An Ab Initio Study. *J. Phys. Chem. C* **2013**, *117*, 22467–22477. [[CrossRef](#)]
20. Meggiolaro, D.; Gigli, G.; Paolone, A.; Reale, P.; Doublet, M.-L.; Brutti, S. Origin of the voltage hysteresis of MgH<sub>2</sub> electrodes in lithium batteries. *J. Phys. Chem. C* **2015**, *119*, 17044–17052. [[CrossRef](#)]
21. Silvestri, L.; Farina, L.; Meggiolaro, D.; Panero, S.; Padella, F.; Brutti, S.; Reale, P. On the reactivity of sodium alanates in lithium batteries. *J. Phys. Chem. C* **2015**. [[CrossRef](#)]
22. Balducci, G.; Brutti, S.; Ciccioli, A.; Gigli, G.; Manfrinetti, P.; Palenzona, A.; Butman, M.; Kudin, L. Thermodynamics of the intermediate phases in the Mg-B system. *J. Phys. Chem. Solids* **2005**, *66*, 292–297. [[CrossRef](#)]
23. Brutti, S.; Colapietro, M.; Balducci, G.; Barba, L.; Manfrinetti, P.; Palenzona, A. Synchrotron powder diffraction Rietveld refinement of MgB<sub>20</sub> crystal structure. *Intermetallics* **2002**, *10*, 811–817. [[CrossRef](#)]
24. Chlopek, K.; Frommen, C.; Leon, A.; Zabara, O.; Fichtner, M. Synthesis and properties of magnesium tetrahydroborate, Mg(BH<sub>4</sub>)<sub>2</sub>. *J. Mater. Chem.* **2007**, *17*, 3496–3503. [[CrossRef](#)]
25. Brutti, S.; Mulas, G.; Piciollo, E.; Panero, S.; Reale, P. Magnesium hydride as high capacity negative electrode for lithium ion batteries. *J. Mater. Chem.* **2012**, *22*, 14531–14537. [[CrossRef](#)]
26. Varin, R.A.; Czujko, T.; Wronski, Z.S. *Nanomaterials for Solid State Hydrogen Storage*; Springer: Cleveland, OH, USA, 2008.
27. Oumellal, Y.; Zlotea, C.; Bastide, S.; Cachet-Vivier, C.; Léonel, E.; Sengmany, S.; Leroy, E.; Aymard, L.; Bonnet, J.-P.; Latroche, M. Bottom-up preparation of MgH<sub>2</sub> nanoparticles with enhanced cycle life stability during electrochemical conversion in Li-ion batteries. *Nanoscale* **2014**, *6*, 14459–14466. [[CrossRef](#)] [[PubMed](#)]
28. Teprovich, J.A., Jr.; Zhang, J.; Colon-Mercado, H.; Cuevas, F.; Peters, B.; Greenway, S.; Zidan, R.; Latroche, M. Li-driven Electrochemical Conversion Reaction of AlH<sub>3</sub>, LiAlH<sub>4</sub>, and NaAlH<sub>4</sub>. *J. Phys. Chem. C* **2015**, *119*, 4666–4674. [[CrossRef](#)]
29. Brutti, S.; Manzi, J.; De Bonis, A.; Di Lecce, D.; Vitucci, F.; Paolone, A.; Trequattrini, F.; Panero, S. Controlled synthesis of LiCoPO<sub>4</sub> by a solvo-thermal method at 220 °C. *Mater. Lett.* **2015**, *145*, 324–327. [[CrossRef](#)]
30. Gentili, V.; Brutti, S.; Hardwick, L.J.; Armstrong, A.R.; Panero, S.; Bruce, P.G. Lithium insertion into Anatase Nanotubes. *Chem. Mater.* **2012**, *24*, 4468–4476.
31. Bonino, F.; Brutti, S.; Piana, M.; Natale, S.; Scrosati, B.; Gherghel, L.; Muller, K. Structural and electrochemical studies of a hexaphenylbenzene pyrolyzed soft carbon as anode material in lithium batteries. *Electrochim. Acta* **2006**, *51*, 3407–3412. [[CrossRef](#)]

